AGU PUBLICATIONS

JGR

Journal of Geophysical Research: Atmospheres

RESEARCH ARTICLE

10.1002/2014JD021738

Key Points:
- Distribution of strokes around initial ones shows a deterministic pattern
- Propose a process that leads to the formation of new lightning channels
- Use 8 years of NLDN and LMA to study breakdown activity around CGs

Correspondence to:
F. G. Zoghzoghy,
fadiz@stanford.edu

Citation:
Zoghzoghy, F. G., M. B. Cohen, R. K. Said, S. S. Basilico, R. J. Blakeslee, and U. S. Inan (2014), Lightning activity following the return stroke, *J. Geophys. Res. Atmos.*, *119*, doi:10.1002/2014JD021738.

Received 10 MAR 2014
Accepted 13 JUN 2014
Accepted article online 18 JUN 2014

Lightning activity following the return stroke

F. G. Zoghzoghy[1], M. B. Cohen[2], R. K. Said[3], S. S. Basilico[1], R. J. Blakeslee[4], and U. S. Inan[1,5]

[1]Department of Electrical Engineering, Stanford University, Stanford, California, USA, [2]School of Electrical and Computer Engineering, Georgia Institute of Technology, Atlanta, Georgia, USA, [3]Vaisala, Inc., Boulder, Colorado, USA, [4]NASA Marshall Space Flight Center, Huntsville, Alabama, USA, [5]Electrical Engineering Department, Koc University, Istanbul, Turkey

Abstract Natural lightning is both frequent and variable and thus a good subject for statistical studies. A typical negative cloud-to-ground (CG) flash consists of multiple individual return strokes. The spatial and temporal distributions of various lightning events throughout the discharge provide a surrogate look inside the CG flash and offer insight into the underlying physical processes. In this study, we combine 8 years of National Lightning Detection Network™ (NLDN) and North Alabama Lightning Mapping Array (NALMA) data to compute the spatial and temporal distributions of (i) subsequent NLDN-reported return strokes and (ii) LMA-reported sources around NLDN-reported CG strokes. Subsequent strokes are separated into those with the same contact point as the first stroke and those flowing along new lightning channels. Statistically, the distribution of strokes along new channels evolves deterministically, with ~200 km/s propagation speed from the original channel, comparable to the speed of a stepped leader. This suggests that the −CG subsequent strokes forming new channels may be directly linked to the initial one by a propagating leader inside the cloud. We present LMA case studies and a multiyear analysis of NLDN-LMA data that support this behavior. Our results are supported by ground-truth measurements and video recordings from previous field studies.

1. Introduction

Approximately four million lightning strikes occur around the globe every day [*Christian et al.*, 2003], but the physical processes underlying this natural phenomenon are not fully understood. Lightning is a powerful electrical discharge that releases billions of joules of energy, neutralizing the charge separation inside a thundercloud [*Rakov and Uman*, 2007, p. 7]. Lightning discharges are of great practical interest to those concerned with the safety of aircrafts, spacecraft, ground-based electronic systems, and their impacts on the power grid. The physical processes are difficult to study due to the wide range of time scales that are involved, the seemingly random nature of lightning processes, and the difficulty of making direct ground-truth measurements inside thunderclouds or inside the lightning channel. However, lightning remains a good candidate for statistical studies due to its abundance in nature.

Lightning processes radiate impulsive electromagnetic waves from DC to optical frequencies, extending to X-rays and gamma rays. The electromagnetic pulse associated with the intense return stroke is known as a radio atmospheric, or sferic for short, and is used as a remote sensing measurement to study and to geolocate lightning. The spectrum of sferics peaks in the very low frequency (VLF; 3–30 kHz) band [*Uman*, 1987, p. 118], where waves propagate efficiently in the so-called Earth-ionosphere waveguide (few dB attenuation per 1000 km). The higher-frequency components decay faster with distance. Various commercial and research-based lightning sensors monitor different frequency bands and are each better at imaging different aspects of lightning. VLF sensors offer global coverage but have limited spatial (several kilometers) and temporal (microseconds) resolution and are sensitive mostly to the return stroke. On the other hand, very high frequency (VHF; 30–300 MHz), ultra high frequency (UHF; 0.3–3 GHz), and optical sensors resolve stepping of the leader channel down to the meter scale but are limited to line of sight coverage.

Several geolocation networks monitor lightning activity around the globe. Our study uses data from the National Lightning Detection Network™ (NLDN) [*Cummins et al.*, 1998; *Cummins and Murphy*, 2009] and the North Alabama Lightning Mapping Array (NALMA) [*Goodman et al.*, 2005]. NLDN, operated by Vaisala, Inc., utilizes VLF and low-frequency (LF; 30–300 kHz) sensors to provide stroke locations with detection efficiency of 90% for cloud-to-ground (CG) flashes and a 308 m median location accuracy within the continental United States [*Nag et al.*, 2011]. NALMA, operated by the NASA Marshall Space Flight Center, the University

of Alabama Huntsville, and New Mexico Tech, uses a dense array of VHF sensors, providing accurate (tens of meters) three-dimensional maps of the lightning activity [*Goodman et al.*, 2005]. However, LMA is limited to line of sight coverage, only collecting lightning data within a few hundred kilometers from the center of the network [*Goodman et al.*, 2005]. While NLDN geolocates lightning strokes using energy radiated by the return stroke, NALMA images intermittent breakdown processes (referred to by the term sources in this work) related to in-cloud or stepped leader activity. The interest in LMA networks has been growing over the past several years as they provide a look inside the thundercloud, enabling intracloud (IC) lightning studies and offering a better understanding of breakdown processes.

The charge inside a lightning-producing cloud typically has a tripole structure, with a positive charge layer at the top, a negative charge layer in the middle, and a smaller positive charge layer at the bottom [*MacGorman and Rust*, 1998, chapter 3]. Most lightning flashes can be classified as either CG or IC. CG flashes account for approximately 25% of lightning activity [*Prentice and Mackerras*, 1977] but are more dangerous to ground assets and can lead to casualties and damages. Approximately 90% of CGs are negative (−CG), initiating in the middle negative charge layer inside the thundercloud [*Jacobson and Krider*, 1976]. A −CG flash typically consists of multiple return stokes separated by tens of milliseconds, each preceded by a lightning leader [*Berger et al.*, 1975; *Rakov and Uman*, 2007, p. 4]. The stepped leader precedes the initial return stroke and travels to ground with an average speed of 200 km/s forming a conductive path in virgin air [*Rakov and Uman*, 1990a]. The stepped leader propagates in intermittent steps, with an average step length of 50 m and an overall duration of tens of milliseconds [*Rakov and Uman*, 1990a], leading to a treelike structure. Once the leader attaches to the ground, the initial return stroke illuminates one of the drawn paths, which has been observed optically to travel upward at one third to one half the speed of light with typical peak currents ranging from a few to many hundreds of kiloamperes.

Subsequent return strokes recur either along the same existing channel (which has an elevated temperature and higher conductivity) via a dart leader or in a newly formed channel up to several kilometers away from the first ground contact point with another stepped leader or a dart-stepped leader [*Rakov and Uman*, 2007, pp. 164–165]. Unlike the stepped leader, the dart leader travels in a more continuous fashion and roughly 2 orders of magnitude faster (total duration of 1–2 ms) due to the higher conductivity of the lingering channel [*Rakov and Uman*, 2007, pp. 164–165]. The dart-stepped leader starts as a dart leader but deviates from the existing channel and continues as a stepped leader, leading to a new ground termination point. Approximately one third of the subsequent strokes exhibit this behavior [*Rakov and Uman*, 1994]. Subsequent strokes are usually separated by tens of milliseconds with J (for "Junction") and K processes occurring between strokes (and after the final one). These processes transport charge from other pockets of charge in the cloud to the top of the ionized channel. K processes are sometimes interpreted as "attempted" leaders that propagate down the existing (but decaying) ionized path but fail to reach ground and do not trigger return strokes [*Rhodes and Krehbiel*, 1989; *Mazur et al.*, 1995].

The remaining 10% of CGs are positive (+CG) and usually consist of a single return stroke followed by continuing currents lasting tens to hundreds of milliseconds [*Rakov and Uman*, 2007, p. 222]. +CGs tend to have higher peak currents and longer current risetimes (compared to −CGs) [*Berger et al.*, 1975]. Unlike negative leaders which are always optically stepped when they propagate in virgin air, positive leaders can move in either a stepped or a continuous fashion. The resulting radiated electromagnetic field waveforms are less likely to exhibit step pulses and do not usually radiate at VHF as strongly as negative leaders [*Rakov and Uman*, 2007, p. 223].

IC flashes account for the remaining 75% of lightning activity and consist of a breakdown process that connects a positive and a negative charge pocket [*Prentice and Mackerras*, 1977]. These flashes tend to dominate the early stages of thunderstorm development [*Rakov and Uman*, 2007, p. 49]. The study of IC lightning is limited due to the difficulty of capturing optical data and the inability to directly measure currents and charge transfers. Thus, IC observations are mostly confined to ground-based remote sensing techniques, using electric, magnetic, or acoustic systems [*Rakov and Uman*, 2007, p. 321].

Many studies have used LMA and other systems to study the formation of the IC lightning channel. *Krider et al.* [1975] was the first to investigate the regular pulse bursts in IC flashes. ICs are composed of two stages, an early/active stage and a late/final stage [*Rakov and Uman*, 2007, p. 322]. The early stage lasts tens to hundreds of milliseconds, consisting of a channel that extends in an intermittent manner with a speed in the order of 100 km/s [*Shao and Krehbiel*, 1996; *Akita et al.*, 2010]. In general, this active stage is similar to the

breakdown process and the propagating stepped leader in −CG flashes [*Rakov and Uman*, 2007, p. 340]. The early stage transitions to the late stage as the connection between the positive and negative charge layers weakens. The late stage transports negative charge from more distant pockets of charge to the location of the discharge. The late stage is also known as the J-type stage due to similarities of the associated physical process to the J process in −CG flashes. The various transient processes throughout the late stage are referred to as K processes and are sometimes called "recoil streamers" [*Rakov and Uman*, 2007, p. 322]. These K processes can retrace the same path several times and lead to steplike field changes known as K changes [*Akita et al.*, 2010]. The observation that many K changes occur with regular pulse bursts suggests that a process similar to the stepped leader in −CG flashes is involved [*Rakov et al.*, 1996].

The stepped leader currents in cloud flashes and the stepped leader currents in ground flashes are comparable [*Proctor*, 1997]. *Shao and Krehbiel* [1996] report that the propagation speeds of initial leaders in ICs and CGs are similar at approximately 100 to 300 km/s. *Proctor* [1981, 1991, 1997] further studies the initial breakdown processes in cloud and ground flashes and shows that CGs only initiate at lower altitudes while ICs originate at both higher and lower altitudes. *Proctor* [1997] also shows that CGs and lower origin ICs have indistinguishable VHF and UHF signatures and that the characteristics of the breakdown in CGs and lower origin ICs "differ in no way that can be detected at Medium Frequency (MF; 0.3–3 MHz), at High Frequency (HF; 3–30 MHz), or at VHF." Further, these studies argue that there is no way of determining a priori whether subsequent stages of a flash following a low-origin breakdown will or will not involve a path to ground.

In this paper, we conduct a multiyear analysis, similar to that of *Zoghzoghy et al.* [2013] and *Finke* [1998] but applied to shorter time scales, to study spatiotemporal patterns of interstroke lightning activity and the statistical linkage between strokes in −CG flashes. We combine 8 years of lightning data from the North Alabama LMA and NLDN to investigate leader propagation inside the cloud throughout CG flashes and to determine the spatial and temporal linkage between −CG strokes. We propose that a −CG stroke can produce a new cloud leader that propagates at lower cloud altitudes, potentially turning into a stepped leader forming a new channel for subsequent strokes. We present case studies that support this behavior and extract features from our multiyear analysis that complement the presented case studies. These advances contribute to the understanding of in-cloud activity in −CG flashes, the development of lightning grouping algorithms, and a more accurate interpretation of LMA readings around ground lightning.

2. Observations

2.1. Description of Data

We analyze lightning data collected by NLDN and NALMA. NLDN geolocates lightning in the continental USA using ∼150 LF sensors spaced by 300–400 km and close enough to the lightning source to detect the ground wave. The NLDN stroke CG detection efficiency is ∼60-80% [*Cummins and Murphy*, 2009] with a median error of 308 m [*Nag et al.*, 2011]. The network tags every detected stroke with a 2-D location (latitude and longitude), a polarity, a peak return stroke current, and a measure of geolocation uncertainty that depends on the number and locations of sensors that detected the event.

The NALMA consists of 11 VHF receivers deployed across northern Alabama and a base station located at the National Space Science and Technology Center in Huntsville, Alabama [*Goodman et al.*, 2005; *White et al.*, 2013]. The system remotely senses the sources of impulsive VHF radio signals from lightning by measuring their time of arrival at the different sensors. Typically, hundreds of LMA sources per flash can be reconstructed, producing accurate 3-D lightning channel image maps (latitude, longitude, and altitude) with ∼50 m location error, within 250 km from the center of the LMA network [*Goodman et al.*, 2005; *White et al.*, 2013].

2.2. Statistical Approach

We use a statistical approach similar to the one of *Zoghzoghy et al.* [2013] and *Finke* [1998] to compute the space-time cross correlation between two groups of lightning events, A and B. Two events a_i and b_j (from group A and group B, respectively) occur around each other (in space and time) based on a probability distribution that is governed by the physics that relate A and B. We compute the empirical space-time occurrence histogram for events in group B around events in group A and inspect the resulting matrix to infer statistical patterns that may provide additional insight into the underlying lightning physics. We calculate overall averages across season, location, and lightning parameters such as peak stroke current, flash multiplicity, and storm phase.

The method presented in Algorithm 1 is used to compute the occurrence histogram $H_{A,B}(\Delta d, \Delta t)$ of events in B (b_j, $j = 1,...,M$) around events in A (a_i, $i = 1,...,N$). To do so, we center a_i at the origin and compute the relative distance Δd_{ij} and time delay Δt_{ij} between a_i and each event b_j in B. We then increment the corresponding histogram entry and repeat this process for all a_i in A, resulting in $H_{A,B}(\Delta d, \Delta t)$. We focus on interstroke lightning processes and only collect pairs of events that fall in our spatial and temporal intervals of interest, $[d_{min}, d_{max}]$ and $[t_{min}, t_{max}]$, respectively.

Algorithm 1 Occurrence Histogram

1: **for** every a_i in group A **do**
2: **for** every b_i in group B **do**
3: Δd_{ij} = distance from $(lat, lon)_{b_j}$ to $(lat, lon)_{a_i}$
4: Δt_{ij} = time delay between b_i and a_i
5: **if** Δd_{ij} in $[d_{min}, d_{max}]$, Δt_{ij} in $[t_{min}, t_{max}]$ **then**
6: increment entry in $H_{A,B}(\Delta d, \Delta t)$
7: **end if**
8: **end for**
9: **end for**

Finke [1998] applies a similar technique to hour time scales to monitor storm motion, as the 2-D histogram H can be thought of as the autocorrelation function of the lightning activity. *Zoghzoghy et al.* [2013] study processes with time scales on the order of tens of seconds to monitor the buildup of the electric fields inside thunderclouds between flashes, using lightning occurrence probabilities as a surrogate measure of electric field intensification. In our study, we apply the statistical approach to the shorter (millisecond) time scales to study interstroke processes in a −CG. In section 2.3, we compute the distribution of (subsequent) NLDN −CG strokes around (initial) NLDN −CG strokes to quantify the impact of a return stroke on subsequent ones, and in section 3.3, we compute the distribution of LMA sources following NLDN −CG strokes to study cloud breakdown processes during −CG discharges.

2.3. Application to NLDN −CG Stroke Data

We apply the statistical approach presented in section 2.2 to all of the NLDN-detected −CGs from July 2010 to study the spatial and temporal distributions of first subsequent −CG strokes following initial −CG strokes. The occurrence histogram is constructed using pairs of events (initial, first subsequent) that occur within 10 km and 1 s time delay. We thus apply Algorithm 2.2 with the following parameters: group A consists of initial −CGs, group B consists of first subsequent −CGs, $N = M = 2{,}033{,}935$ strokes, $d_{min} = 0$, $d_{max} = 10$ km, $t_{min} = 0$, and $t_{max} = 1$ s. We only use −CG data with peak currents stronger than −15 kA to minimize the population of mislabeled IC strokes [*Cummins and Murphy*, 2009].

The histogram values are scaled by their corresponding bin area (more distant bins map to larger physical regions), and the summation over all the histogram values is normalized to unity. The resulting (normalized) space-time occurrence distribution of first subsequent strokes around initial −CGs is shown in Figure 1. The radial distances Δd are binned into 100 m bins, and the relative time delays Δt are in 4 ms bins.

Two features stand out in Figure 1: (i) a horizontal feature that extends in time (up to 800 ms) dominated by events that are within ∼750 m and (ii) a vertical (but slightly tilted) feature that extends from 1 km to 7 km. The horizontal feature corresponds to subsequent strokes that recur along the existing ground channel (EGC). EGCs occur in the same location as the initial return stroke but the EGC feature appears to have a nonzero spatial width due to the NLDN geolocation error (two strokes that occur in the same channel should have the same location). We note that the EGC feature also includes subsequent events that follow dart-stepped leaders that deviate from the initial channel at lower altitudes (0.7–3.5 km) and contact the ground within 750 m. These events affect the spatial and temporal shapes of the EGC feature.

The second feature corresponds to subsequent strokes that create a new ground channel (NGCs) 1–7 km away from the location of the initial channel. The ability to visually separate between the two features is consistent with ground-truth video recordings that show that NLDN can identify the different channel locations

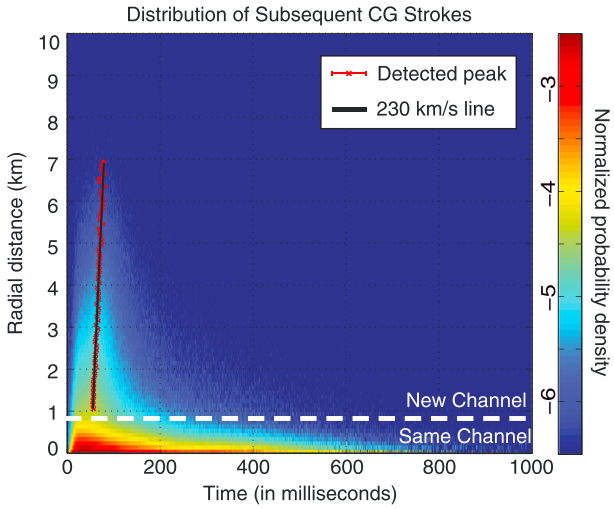

Figure 1. Spatial and temporal distributions of subsequent strokes around initial strokes, using 2,033,935 NLDN −CG strokes from July 2010. The histogram is scaled by the differential area of each radius bin, the summation over the histogram entries is normalized to unity, and the resulting values are displayed (color coded) on a logarithmic scale. The white dashed line corresponds to a radial distance of 750 m, marking an approximate separation between the NLDN-reported location of subsequent strokes that recur along the same channel and the reported location of strokes that form a new one [*Stall et al.*, 2009]. The solid black line corresponds to the least squares linear fit through the peaks of lightning occurrence as a function of radial distance.

in a −CG discharge with a separation criterion of about 1 km throughout most of the United States [*Stall et al.*, 2009]. *Stall et al.* [2009] finds the mean horizontal separation between first and other subsequent strokes to be 2.3 ± 1.7 km (59 observations). *Thottappillil et al.* [1992] use video recordings to compute the distances between all different pairs of contacts in 22 CG flashes and find an average spatial separation of 1.7 km and a maximum separation of 7.3 km. *Ishii et al.* [1998] observe that the spatial extent of a flash can be as large as 10 km for −CG flashes with an average of 2.1 km (40 observations). Multistroke flashes and the spatial separation between subsequent strokes are important for both lightning attachment physics and for lightning safety and protection systems and are an active field of research [*Fleenor et al.*, 2009; *Saba et al.*, 2010; *Ballarotti et al.*, 2012].

We note that NLDN could miss the first subsequent stroke and detect a later one due to the 60–80% network stroke detection efficiency [*Cummins and Murphy*, 2009; *Nag et al.*, 2011]. Thus, these invalid pairs of events occur later in time and add a right tail (in time) to the EGC and NGC features. However, their effect should be minimal for a large sample size.

Roughly half of the first subsequent strokes are NGCs and the other half EGCs. We follow the same approach to study (i) the spatial and temporal distributions of second subsequent strokes around first subsequent strokes and (ii) the distribution of third subsequents around second subsequents. The resulting distributions are (visually) similar to the one presented in Figure 1 showing both the NGC and the EGC features. However, the proportion of EGC events increases from 49% for first subsequent strokes (following initials) to 60% for second subsequents (following first subsequents) and to 68% for third subsequents (following second subsequents), suggesting that higher-order subsequent strokes are more likely to recur along the preceding channel. These proportions are consistent with various ground-truth studies [*Stall et al.*, 2009; *Rakov and Uman*, 1990b; *Rakov et al.*, 1994; *Valine and Krider*, 2002; *Saba et al.*, 2006]. Although the proportion of NGCs and EGCs varies between these field studies (mostly due to the limited sample size), the authors suggest that the first subsequent stroke in a −CG flash is more likely to produce a new ground termination.

To further study higher-order return strokes, we apply our analysis to −CG data from July to August 2011 and compare flashes with three strokes in the same location to flashes with three strokes in three different locations. For the former, 18% of next subsequent strokes form a new channel, but for the latter, it is 48%. As a channel has been repeatedly conditioned with strokes, the probability of a new channel being formed decreases. Our results suggest that new channels are more likely to form when the preceding stroke also occurs in a new location with a stepped leader.

The vertical NGC feature is characterized with a (roughly) constant speed. We determine this speed as follows: In each distance bin of the histogram, we first apply a 20 ms moving average window to smooth the histogram entries as a function of time, resulting in $H^{*}_{\mathrm{A,B}}(\Delta d, \Delta t)$ and then find the peak time delay $\Delta t_i^{\mathrm{peak}}$ as shown in equation (1). We repeat the process for all distances between 1 and 7 km. The peaks are shown in red. The black line is a least squares regression fitline: $\mathbf{\Theta_{ls}} = (\mathbf{X}^T\mathbf{X})^{-1}\mathbf{X}^T\mathbf{Y}$, where $x_i = \Delta t_i^{\mathrm{peak}}$ and $y_i = r_i$, and $\Delta t_i^{\mathrm{peak}}$ is given by

$$\Delta t_i^{\mathrm{peak}} = \arg\max_{\Delta t} H^{*}_{\mathrm{A,B}}(\Delta d = r_i, \Delta t) \quad (1)$$

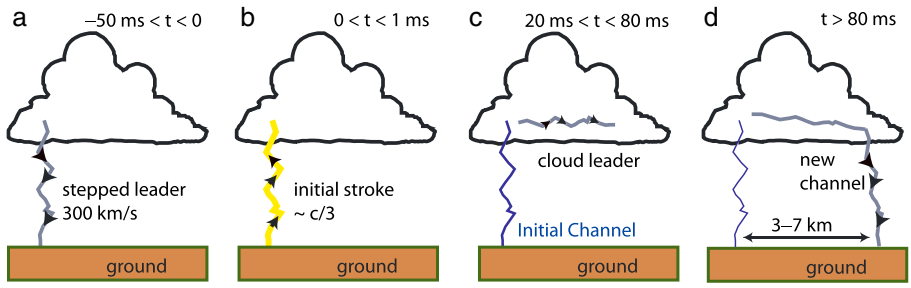

Figure 2. Cartoon of the suggested physical process that governs the formation of distant subsequent channels in −CG flashes. (a) A stepped leader propagates downward at a speed of 100–300 km/s to form an initial channel. (b) The return stroke propagates upward along the ionized channel at ~c/3. (c) A leader follows the return stroke propagating outward in the cloud. (d) The cloud leader turns into a downward stepped leader and forms a new lightning channel 3–7 km from the location of the initial one.

Our results suggest that the peak −CG activity around the initial stroke is moving outward at a speed of ~ 230 km/s. For instance, a subsequent stroke occurring 5 km away from the initial stroke is most likely to occur after ~77 ms delay. We repeat this analysis for three separate months of NLDN data (August 2010, July 2011, and August 2011) and find the slope of the NGC feature to vary between 200 and 280 km/s, so it is possible that there is some variation by storm type and season. These speeds are comparable to the speed of the stepped leader reported by *Rakov and Uman* [2007, p. 123] and to the 100–200 km/s speeds measured by *Mazur et al.* [1995] and *Montanya et al.* [2014] using high-speed video recordings.

It is believed that the formation of a new ground contact point follows a dart-stepped leader. *Davis* [1999] shows that dart-stepped leaders deviate from the existing channel at heights of 0.7 to 3.4 km then travel to ground at typical speed of 100–300 km/s. This mechanism is consistent with the observed speed of the NGC feature but is unlikely to explain the formation of new ground terminations with 4–10 km separation distances (supported by the aforementioned field studies) as the dart-stepped leader would have to propagate horizontally for several kilometers after it branches out at 0.7–3.4 km heights. We propose another mechanism in section 3.1 that could potentially explain NGCs that form with separation distances as large as the ones observed.

3. Discussion

3.1. Proposed Mechanism

Proctor [1981, 1997] uses VHF and UHF imaging systems to study cloud discharges and suggests that horizontal ICs follow a horizontally propagating cloud stepped leader. The two studies describe four lower origin horizontal ICs following horizontal leaders and claim that stepped leaders in lower origin ICs are indistinguishable from the stepped leader in CGs. Additionally, the author argues that there is no way of determining a priori whether the flash following a low-origin breakdown will or will not involve a path to ground.

The cartoons shown in Figure 2 present a lightning mechanism that could potentially explain our observations. Figures 2a and 2b illustrate the initial stepped leader which precedes the initial CG return stroke, producing a conductive channel in virgin air. Following the CG stroke, we propose that in-cloud leaders could form at the tip of the lightning channel, propagating horizontally in the cloud, as shown in Figure 2c. The cloud leader could then grow into a second cloud-to-ground stepped leader, producing a new ground termination several kilometers away from the previously existing one. The proposed mechanism could explain the deterministic linkage between distant return strokes within the same −CG discharge.

Previous observations and studies support this mechanism and offer similar physical explanations. *Montanya et al.* [2014] observe a ground-to-cloud-to-ground flash which initiates as an upward negative leader with a 100 km/s propagation speed. The leader then branches out in the cloud into negative and positive leaders (at 5–6 km altitude) and turns into a stepped leader producing a −CG several kilometers from the initiation point. *Mazur et al.* [1995] studies a negative CG flash consisting of six return strokes using high-speed video recordings, a VHF interferometer, and electric, magnetic, and optical sensors and observe that the first subsequent return stroke occurs in a new channel following a stepped leader that initiated from the location of the initial channel.

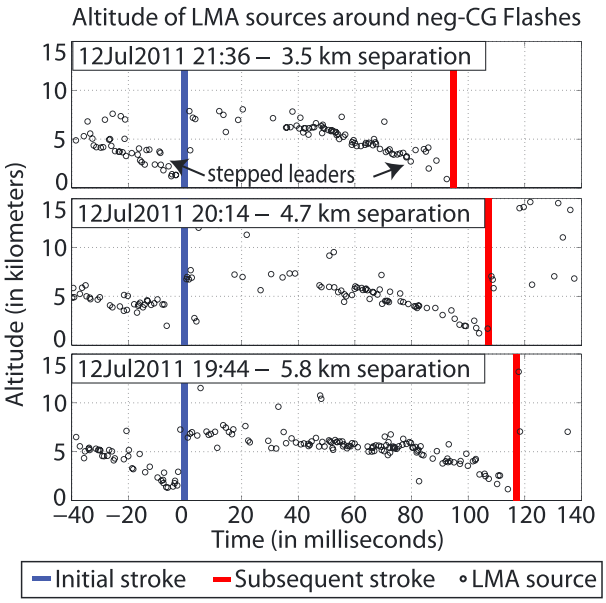

Figure 3. Case studies of the occurrence of North Alabama LMA sources coincident with NLDN −CG return strokes. (top, middle, and bottom) −CG flashes, showing the altitude of LMA sources as a function of time relative to the initial NLDN stroke. The times of the initial and subsequent strokes are displayed in blue and red, respectively.

Krehbiel [1981] offers a physical explanation for the formation of new channels using electric field data from multiple-channel −CGs and finds that new channels are preceded by strokes that have a cutoff along the lower extent of the channel. The resulting deposition of negative charge along the channel (above the cutoff) could lead the subsequent leader to follow a different path to ground. The author notes that the cutoff field changes are most pronounced after strokes initiated by stepped leaders, which is consistent with our results from section 2.3.

Next, we use NALMA 3-D maps of VHF sources to image the intermittent breakdown activity inside the cloud throughout −CG flashes to observe the signature of the proposed mechanism.

3.2. LMA Case Studies

Figure 3 consists of three NLDN −CG flashes from 12 July 2011 with overlayed NALMA data. The altitude of the LMA sources is plotted as a function of time delay relative to the initial NLDN return stroke. All three −CG flashes consist of an initial and a subsequent stroke. For visual reference, we draw two vertical lines, one in blue and another in red, to highlight the time of the initial and first subsequent stroke, respectively. The NLDN-reported separation between the strokes is 3.5 km (Figure 3, top), 4.7 km (Figure 3, middle), and 5.8 km (Figure 3, bottom), suggesting that these subsequent strokes occur in new channels. The separation distances are well above the median geolocation error and are consistent with the LMA locations. We only include LMA events that occurred within a 10 km horizontal range around the location of the initial stroke, ensuring that the LMA-detected sources are predominantly related to the intermittent interstroke activity (corresponding to that flash).

All three initial strokes are followed by VHF activity inside the cloud at altitudes near 5 km. The intermittent activity then grows into a stepped leader preceding the NGC. The presence of VHF radiation as the leader propagates to ground suggests that the leader descends in a stepped-like fashion, forming a new channel in virgin air (dart leaders are nearly invisible in VHF). Figure 3 shows that all three NGCs do not follow dart-stepped leaders and are likely due to a mechanism consistent with the one proposed in section 3.1.

In addition, Figure 3 suggests that more distant NGCs have longer interstroke time delays. The separation distances and interstroke time delays are (3.5 km, 95 ms), (4.7 km, 107 ms), and (5.8 km, 117 ms) for the top, middle, and bottom, respectively. This suggests the presence of a feature that propagates away from the location of the initial stroke at an average speed ~110 km/s, taking more time to reach greater separation distances. To better observe this effect, we investigate the 3-D distribution of LMA sources as a function of time throughout the flash.

Figure 4 provides a top-down view (top) and a side view (bottom) of the −CG flash from Figure 3 (bottom). The top-down view shows the 2-D location (latitude and longitude) of the LMA sources color coded in time. The side view shows the altitude of the sources throughout the duration of the flash. Both panels use the same color coding scale, with a reference time corresponding to the onset of the initial return stroke (shown in blue). The locations of the initial and subsequent strokes are marked in both panels in blue and in red, respectively.

The top-down view reveals that interstroke LMA sources initially occur around the location of the existing channel and then propagate away to the location of the new one. The majority of the horizontal

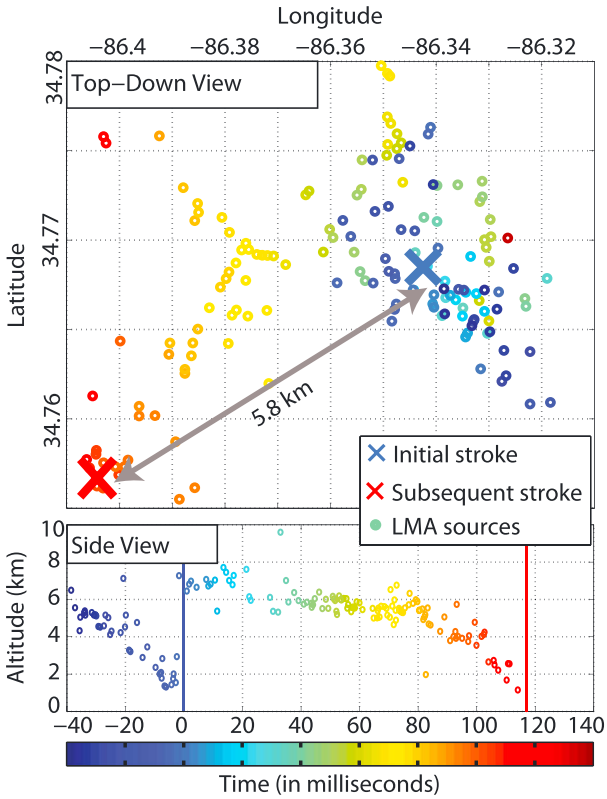

Figure 4. (top) Top-down view of an NLDN −CG flash with overlayed LMA sources, color coded in time relative to the initial stroke (blue). (bottom) Side view of the same −CG flash, showing the altitude of sources as a function of time color coded in time consistent with Figure 4, top. The event occurred on 12 July 2011 at 19:44 UT.

propagation occurs within the cloud (green to orange sources ~40–80 ms) at an altitude of ~5 km. The leader propagates downward to form an NGC 5.8 km away. The LMA sources form a typical stepped leader VHF signature; the dart-stepped leader is unlikely to produce such observations.

Both Figures 3 and 4 provide evidence that the initial return stroke could potentially lead to a new stepped leader, initially at the tip of the preexisting channel, which propagates horizontally in the cloud and then downward to create an NGC. We inspect 980 multichannel NLDN −CG flashes (NGCs) that occur within 150 km from the center of NALMA from 8 to 14 July 2011. Roughly 230 flashes have LMA sources, but only 34 are close enough to the sensors and have VHF sources (that propagate to ground) corresponding to the initial stepped leader. We find that half of these flashes (17 out of 34) exhibit a behavior similar to the one shown in Figure 4. The remaining cases do not show a clear (or any) connection between the two lightning channels.

In the following section, we explore this with much larger statistics with multiple years of LMA and NLDN data, to characterize the (horizontal) space-time distribution of sources around initial NLDN −CG strokes.

3.3. Application to LMA Data Around NLDN −CG

We apply the same technique to NLDN −CG stroke data and NALMA data from 2004 to 2010. We only select initial −CG events that occur within 200 km from the center of the NALMA array and that lead to subsequent NGCs. We compute the space-time distribution of in-cloud LMA sources following initial strokes, using LMA sources with altitudes above 4 km. Our aim is to extract the average behavior of sources inside the cloud throughout a multichannel −CG. The 2-D histogram is computed using pairs of events (initial strokes, LMA sources) that occur within 10 km (horizontal distance) and 1 s time delay. We thus apply Algorithm 2.2 with the following parameters: group A consists of all 2004–2010 initial −CG strokes leading to a NGC within 200 km from the LMA center, group B consists of all 2004–2010 LMA sources above 4 km, $d_{min} = 0$, $d_{max} =$ 10 km, $t_{min} = 0$, and $t_{max} = 1$ s. As previously mentioned we only use −CG data with peak currents stronger than −15 kA [*Cummins and Murphy*, 2009].

Figure 5 shows the occurrence rate of in-cloud LMA sources around initial −CGs as a function of time, parameterized by separation distance. We divide the region around the initial stroke into concentric regions with 1 km increments and compute the occurrence of LMA sources in each region as a function of time delay with a 100 μs resolution and display the corresponding five-point moving average. We note that the majority of the LMA sources correspond to negative leaders because (i) negative leaders radiate stronger VHF than positive ones and (ii) we focus our analysis on −CGs. Since we are only interested in comparing the shapes of the curves, we normalize them to unit area (that is, we are not interested in the absolute values of the peaks). The time is displayed on a logarithmic scale to highlight features with a wide range of time scales. We use

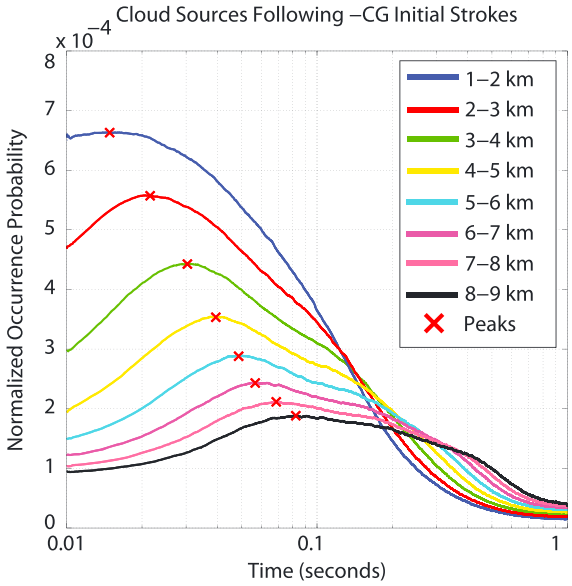

Figure 5. Temporal distribution of LMA sources around NLDN strokes, parameterized by distance, using NLDN and LMA data from 2004 to 2010. The curves are normalized to have unit area and are displayed on a logarithmic time scale.

a method similar to the one presented in equation (1) to find the peak occurrence rate for each curve and display it with a red X symbol.

The results in Figure 5 suggest that the distribution of the relative location of cloud sources propagates outward, with an expanding radial envelope. The rate of occurrence peaks in the 1–2 km region (in blue) after 14.9 ms, in the 4–5 km region (in yellow) after 39.4 ms, and in the 7–8 km region (in magenta) after 68.8 ms. The horizontal propagation of the cloud LMA occurrence distribution is in agreement with our case study observations and further supports the mechanism proposed in section 3.1. The average extracted leader speed is ~110 km/s, consistent with ground-truth measurements of cloud leader activity [*Shao and Krehbiel*, 1996; *Akita et al.*, 2010]. The speed of the cloud leader is on the lower end of the 100–300 km/s range of stepped leader speeds [*Rakov and Uman*, 2007, p. 123] and is comparable to the speed of the intermittent breakdown process in the early stage of the horizontal cloud discharge [*Shao and Krehbiel*, 1996; *Akita et al.*, 2010]. We note that the LMA-extracted 110 km/s speed for cloud leader propagation is slower than the 200–280 km/s observed using NLDN return stroke data in section 2.3. There are several reasons that could explain the difference between the resulting speeds. We suggest two: (i) the faster dart-stepped leaders contribute to the NLDN spatiotemporal statistics but do not contribute to the LMA statistics as dart-stepped leaders do not generate cloud VHF sources and (ii) the speed of the stepped leader increases as the leader approaches ground; recent high-speed camera (1000 frames per second) measurements by *Kong et al.* [2007] show that the speed of a single positive leader increases from 10 km/s to 380 km/s during its descent.

The LMA activity in the 1–2 km region (in blue) appears to have a normal distribution on a logarithmic time scale, which translates into a lognormal distribution (for linear time) of leader time of arrival. In the more distant 4–5 km region (in yellow), the time of arrival distribution and its peak shift (to the right) due to leader propagation delay and the spread of the distribution increases. The 90–10% fall time roughly doubles from 279 ms at 1–2 km to 575 ms at 4–5 km. The larger spread at larger distances results from the randomness in leader growth and propagation, similar to the behavior of a random walk where the variance increases linearly with time. In a recent study, *Campos et al.* [2014] use video recordings to compute the leader speeds and finds that the speed of dart leaders follows a lognormal distribution. Our method could be extended (i) to empirically study the stepped leader speed distribution and (ii) to compute the change in the speed of the stepped leader as it approaches ground. These are important to stepped leader growth models but are beyond the scope of this paper.

The results of the multiyear statistical analysis support the proposed mechanism for the deterministic distribution evolution of new ground terminations. We repeat the same study for single-stroke −CG flashes and find that cloud leaders also follow single-stroke flashes, propagating horizontally in the cloud without approaching ground. Our findings provide new insight into interstroke lightning physics and are relevant to various lightning applications. The quantified space-time evolution and spatial reach of the −CG flash is of particular interest to those interested in lightning prediction and protection systems. The observations are also important for the correct interpretation of lightning data around −CG discharges, namely LMA data and data collected using optical sensors such as the Lightning Imaging Sensor.

4. Conclusion

In this paper, we combine 8 years of data from the North Alabama LMA and NLDN to study the impact of the return stroke on the surrounding lightning activity. The statistical linkage between return strokes suggests that the −CG subsequent strokes forming new channels are directly linked to the initial one by a propagating leader with a speed of ∼200 km/s, and we use LMA case studies and previous ground-truth field experiments to support our findings. We find that new channels are less likely to form for higher stroke orders and are more likely to be preceded by a stepped leader return stroke.

We have repeated our analysis for +CGs, but the relatively rare occurrence of multistroke positive flashes (∼100× fewer in the NLDN data set) and the weak VHF radiation of positive leaders [*Rakov and Uman*, 2007, p. 223] limited our ability to draw an analogous conclusion for these events.

Our findings contribute to the understanding and interpretation of cloud activity in −CG flashes, the development of lightning grouping algorithms, and the tuning of stepped leader growth models. We find that 97% of first subsequent strokes occur within 5.8 km and 750 ms from the initial stroke and that 97% of third subsequents occur within 5.3 km and 750 ms from the second subsequent stroke. These clustering parameters could be used to develop a stroke-to-flash grouping algorithm that uses information such as stroke order and number of preexisting channels.

The statistical method could be further applied to study the speed of the stepped leader as it approaches ground and the change in the space-time distribution of strokes based on lightning parameters (such as stroke order, storm phase, and geographical location) and to study the linkage between spatially separated storm systems.

Acknowledgments

This work is supported by the Defense Advanced Research Project Agency under grant HR0011-10-1-0058-P00001 to Stanford University with subcontract to the Georgia Institute of Technology. NLDN data are provided by Vaisala, Inc. (Ron Holle ron.holle@vaisala.com). The point of contact for NALMA data is Richard Blakeslee (rich.blakeslee@nasa.gov).

References

Akita, M., Y. Nakamura, S. Yoshida, T. Morimoto, T. Ushio, Z. Kawasaki, and D. Wang (2010), What occurs in K process of cloud flashes?, *J. Geophys. Res.*, *115*, D07106, doi:10.1029/2009JD012016.

Ballarotti, M. G., C. Medeiros, M. F. Saba, W. Schulz, and O. J. Pinto (2012), Frequency distributions of some parameters of negative downward lightning flashes based on accurate-stroke-count studies, *J. Geophys. Res.*, *117*, D06112, doi:10.1029/2011JD017135.

Berger, K., R. Anderson, and H. Kroninger (1975), Parameters of lightning flashes, *Electra*, *80*, 223–237.

Campos, L. S., M. F. Saba, T. A. Warner, O. Pinto Jr., E. P. Krider, and R. E. Orville (2014), High-speed video observations of natural cloud-to-ground lightning leaders—A statistical analysis, *Atmos. Res.*, *135-136*, 285–305, doi:10.1016/j.atmosres.2012.12.011.

Christian, H. J., et al. (2003), Global frequency and distribution of lightning as observed from space by the Optical Transient Detector, *J. Geophys. Res.*, *108*(D1), 4005, doi:10.1029/2002JD002347.

Cummins, K. L., and M. J. Murphy (2009), An overview of lightning locating systems: History, techniques, and data uses, with an in-depth look at the U. S. NLDN, *IEEE Trans. Electromagn. Compat.*, *51*(3), 499–518.

Cummins, K. L., M. J. Murphy, E. A. Bardo, W. L. Hiscox, R. B. Pyle, and A. E. Pifer (1998), A combined TOA/MDF technology upgrade of the U. S. National Lightning Detection Network, *J. Geophys. Res.*, *103*, 9035–9044.

Davis, S. M. (1999), Properties of lightning discharges from multiple-station wideband electric field measurements, PhD thesis, Univ. of Florida, Gainesville.

Finke, U. (1998), Space-time correlations of lightning distributions, *Mon. Weather Rev.*, *127*, 1850–1861.

Fleenor, S. A., C. J. Biagi, K. L. Cummins, E. P. Krider, and X. Shao (2009), Characteristics of cloud-to-ground lightning in warm-season thunderstorms in the Central Great Plains, *Atmos. Res.*, *91*, 333–352.

Goodman, S. J., et al. (2005), The North Alabama Lightning Mapping array: Recent severe storm observations and future prospects, *Atmos. Res.*, *76*, 423–437, doi:10.1016/j.atmosres.2004.11.035.

Ishii, M., K. Shimizu, J. Hojo, and K. Shinjo (1998), Termination of multiple-stroke flashes observed by electromagnetic field, paper presented at 24th International Conference on Lightning Protection, Staffordshire Univ., Birminghan, U. K.

Jacobson, E. A., and E. P. Krider (1976), Electrostatic field changes produced by Florida lightning, *J. Atmos. Sci.*, *33*, 113–117.

Kong, X., X. Qie, and Y. Zhao (2007), Characteristics of a positive cloud-to-ground lightning flash observed by high-speed video camera, paper presented at 13th International Conference on Atmospheric Electricity, ICAE, Beijing, China.

Krehbiel, P. R. (1981), An analysis of the electric field change produced by lightning, PhD thesis, Univ. of Manchester Inst. of Sci. and Technol., Manchester, England.

Krider, E. P., G. J. Radda, and R. C. Noggle (1975), Regular radiation field pulses produced by intracloud lightning discharges, *J. Geophys. Res.*, *80*(27), 3801–3804, doi:10.1029/JC080i027p03801.

MacGorman, D. R., and W. D. Rust (1998), *The Electrical Nature of Storms*, Oxford Univ. Press, Oxford, U. K.

Mazur, V., P. R. Krehbiel, and X. M. Shao (1995), Correlated high-speed video and radio interferometric observations of a cloud-to-ground lightning flash, *J. Geophys. Res.*, *100*, 25,731–25,753.

Montanya, J., O. Van Der Velde, and E. R. Williams (2014), Lightning discharges produced by wind turbines, *J. Geophys. Res. Atmos.*, *119*, 1455–1462, doi:10.1002/2013JD020225.

Nag, A., et al. (2011), Evaluation of U. S. National Lightning Detection Network performance characteristics using rocket-triggered lightning data acquired in 2004–2009, *J. Geophys. Res.*, *116*, D02123, doi:10.1029/2010JD014929.

Prentice, S. A., and D. Mackerras (1977), The ratio of cloud to cloud-ground lightning flashes in thunderstorms, *J. Appl. Meteorol.*, *16*, 545–550, doi:10.1175/1520-0450(1977)016<0545:TROCTC>2.0.CO;2.

Proctor, D. E. (1981), VHF radio pictures of cloud flashes, *J. Geophys. Res.*, *86*(C5), 4041–4071, doi:10.1029/JC086iC05p04041.

Proctor, D. E. (1991), Regions where lightning flashes began, *J. Geophys. Res.*, *96*(D3), 5099–5112, doi:10.1029/90JD02120.

Proctor, D. E. (1997), Lightning flashes with high origins, *J. Geophys. Res.*, *102*(D2), 1693–1706, doi:10.1029/96JD02635.

Rakov, V. A., and M. A. Uman (1990a), Waveforms of first and subsequent leaders in negative lightning flashes, *J. Geophys. Res.*, *95*(D10), 16,561–16,577, doi:10.1029/JD095iD10p16561.

Rakov, V. A., and M. A. Uman (1990b), Some properties of negative cloud-to-ground lightning flashes versus stroke order, *J. Geophys. Res.*, *95*(D5), 5447–5453, doi:10.1029/JD095iD05p05447.

Rakov, V. A., and M. A. Uman (1994), Origin of lightning electric field signatures showing two return-stroke waveforms separated in time by a millisecond or less, *J. Geophys. Res.*, *99*(D4), 8157–8165, doi:10.1029/94JD00165.

Rakov, V. A., and M. A. Uman (2007), *Lightning: Physics and Effects*, Cambridge Univ. Press, Cambridge, England.

Rakov, V. A., M. A. Uman, and R. Thottappillil (1994), Review of lightning properties from electric field and TV observations, *J. Geophys. Res.*, *99*(D5), 10,745–10,750, doi:10.1029/93JD01205.

Rakov, V. A., M. A. Uman, G. R. Hoffman, M. W. Masters, and M. Brook (1996), Bursts of pulses in lightning electromagnetic radiation: Observations and implications for lightning test standards, *IEEE Trans. Electromagn. Compat.*, *38*, 156–164, doi:10.1109/15.494618.

Rhodes, C., and P. R. Krehbiel (1989), Interferometric observations of a single stroke cloud-to-ground flash, *Geophys. Res. Lett.*, *16*, 1169–1172.

Saba, M. F., M. G. Ballarotti, and O. Pinto Jr. (2006), Negative cloud-to-ground lightning properties from high-speed video observations, *J. Geophys. Res.*, *111*, D03101, doi:10.1029/2005JD006415.

Saba, M. F., W. Schulz, T. A. Warner, L. S. Campos, C. Schumann, E. P. Krider, K. L. Cummins, and R. E. Orville (2010), High-speed video observations of positive lightning flashes to ground, *J. Geophys. Res.*, *115*, D24201, doi:10.1029/2010JD014330.

Shao, X. M., and P. R. Krehbiel (1996), The spatial and temporal development of intracloud lightning, *J. Geophys. Res.*, *101*(D21), 26,641–26,668, doi:10.1029/96JD01803.

Stall, C. A., K. L. Cummins, E. P. Krider, and J. A. Cramer (2009), Detecting multiple ground contacts in cloud-to-ground lightning flashes, *J. Atmos. Oceanic Technol.*, *26*, 2392–2402.

Thottappillil, R., V. A. Rakov, M. A. Uman, W. H. Beasley, M. J. Master, and D. V. Shelukhin (1992), Lightning subsequent-stroke electric field peak greater than the first stroke peak and multiple ground terminations, *J. Geophys. Res.*, *97*(D7), 7503–7509, doi:10.1029/92JD00557.

Uman, M. A. (1987), *The Lightning Discharge*, Dover, Mineola, New York.

Valine, W. C., and E. P. Krider (2002), Statistics and characteristics of cloud-to-ground lightning with multiple ground contacts, *J. Geophys. Res.*, *107*(D20), 4441, doi:10.1029/2001JD001360.

White, K. D., G. T. Stano, and B. Carcione (2013), An investigation of North Alabama Lightning Mapping array data and usage in the real-time operational warning environment during the March 2, 2012 severe weather outbreak in northern Alabama, paper presented at 93rd American Meteorological Society Annual Meeting, Austin, Tex.

Zoghzoghy, F. G., M. B. Cohen, R. K. Said, and U. S. Inan (2013), Statistical patterns in the location of natural lightning, *J. Geophys. Res. Atmos.*, *118*, 787–796, doi:10.1002/jgrd.50107.